Potential Vorticity Distribution in the North Pacific

LYNNE D. TALLEY

Scripps Institution of Oceanography, University of California, San Diego, La Jolla, California

(Manuscript received 28 August 1986, in final form 20 July 1987)

ABSTRACT

Vertical sections and maps of potential vorticity $\rho^{-1} f \partial\rho/\partial z$ for the North Pacific are presented. On shallow isopycnals, high potential vorticity is found in the tropics, subpolar gyre, and along the eastern boundary of the subtropical gyre, all associated with Ekman upwelling. Low potential vorticity is found in the western subtropical gyre (subtropical mode water), in a separate patch near the sea surface in the eastern subtropical gyre and extending around the gyre, and near sea-surface outcrops in the subpolar gyre; the last is analogous to the subpolar mode water of the North Atlantic and Southern Ocean.

Meridional gradients of potential vorticity are high between the subtropical and subpolar gyres at densities which outcrop only in the subpolar gyre; lateral gradients of potential vorticity are low in large regions of the subtropical gyre on these isopycnals. On slightly denser isopycnals which do not outcrop in the North Pacific, there are large regions of low potential vorticity gradients which cross the subtropical-subpolar gyre boundary. These regions decrease in area with depth and vanish between 2500 and 3000 meters. Regions of low lateral gradients of potential vorticity are surrounded by and overlie regions where the meridional gradient of potential vorticity is approximately β. In the abyssal waters, below 3500 meters, meridional potential vorticity gradients again decrease, perhaps associated with slow geothermal heating. The depth and shape of the region where potential vorticity is relatively uniform or possesses closed contours is noted and related to theories of wind-driven circulation.

1. Introduction

Potential vorticity has recently been found useful in studies of ocean circulation, both as a tracer where strong sources create potential vorticity extrema (Talley and Raymer, 1982; Talley and McCartney, 1982; McCartney, 1982) and because its distribution is one of the clearest points of contact with general circulation theories (e.g. Luyten et al., 1983; Rhines and Young, 1982). In an ideal fluid, potential vorticity is a conserved quantity; in forced, diffusive flow in the parameter range appropriate for ocean circulation, the fundamental equation governing the evolution of flow is the potential vorticity equation. The form of potential vorticity which is used for tracing large-scale circulation ignores the relative vorticity contribution, which we are as incapable of calculating as the absolute velocity field; scaling indicates that this simplification is appropriate except in the region of strong flows. Given that potential vorticity is neither conserved nor passive, it would appear that it is not a very clean tracer; however, its direct relation to forcing, its differences from other tracers and its identity as the field which is predicted by circulation theories make it extremely attractive.

The distribution of potential vorticity in the North Pacific is examined in some detail in the present paper. Since, of all oceans, the North Pacific has the least input of convectively formed water masses and hence a relative lack of strong buoyancy sources of potential vorticity, it is an excellent place in which to compare observations with recent theories of wind-driven circulation. Based on the observations, hitherto unremarked features of the circulation and water mass distribution in the North Pacific are exposed. The observations can be combined with those of other tracers in order to improve interpretation of the potential vorticity field. The potential vorticity field is also compared with results of recent theories of ocean circulation which, despite their incomplete physics and evolutionary state, provide a useful basis for interpreting the potential vorticity observations; the observations in turn can provide a basis for expansion or change in the theories.

The theories of Luyten et al., (1983), Rhines and Young (1982), and the substantial subsequent literature are the most obvious points for comparison with observations. In Luyten et al.'s paper concerning the theory of inviscid circulation in layers which outcrop, regions and patterns of ventilated and unventilated flow were predicted and compared with observations in the North Atlantic; comparisons have also been made with other observations in the North Atlantic (Jenkins, 1987), with observations in the North Pacific (Talley, 1985) and the South Pacific (deSzoeke, 1987), and with

Corresponding author address: Dr. Lynne D. Talley, Mail Code A-030, Scripps Institution of Oceanography, La Jolla, CA 92093.

© 1988 American Meteorological Society

the full outcropping layer of the world ocean (Keffer, 1985). Rhines and Young's (1982) theory and subsequent related papers treat the weakly diffusive, wind-driven circulation in wholly unventilated layers—that is, layers which do not outcrop at all. They showed that circulation can only occur in regions of closed streamlines and that potential vorticity within such regions should be homogenized by weak lateral diffusion. Their theory is strongly supported by observations and numerical models (McDowell et al., 1982; Keffer, 1985; Holland et al., 1984). The major pieces missing from these models for comparison with observations are an exploration of varying amounts of diffusion and the inclusion of thermohaline circulation.

Potential vorticity observations for the North Pacific have been presented previously by Coats (1981), Keffer (1985), and Talley (1985). Coats calculated potential vorticity at a single location in the subtropical gyre in order to apply the β-spiral method of estimating absolute velocities; he found that potential vorticity is uniform on isopycnals at that location between 400 and 1300 meters. Keffer (1985) presented maps of potential vorticity for the world ocean which exposed a number of the essential features of the ventilated parts of the gyres and of the unventilated upper ocean. In Talley (1985), the ventilated portion of the subtropical North Pacific was compared with the model of Luyten et al. (1983); finer slices were used than in Keffer (1985) to study the vertical structure of the ventilated circulation. The present work extends the previous analysis to additional layers and to the abyssal ocean, exposing the vertical structure of both the ventilated and unventilated, wind-driven circulation and of the abyssal circulation. New features of the North Pacific's subtropical and subpolar gyres are found here that correspond with features in other oceans. The vertical and horizontal extent of a large region of homogenized potential vorticity, first identified by Keffer (1985), is explored and identified with the theoretical limits of the wind-driven circulation. Potential vorticity for the abyssal waters is shown for the first time. Zonal averages of potential vorticity on isopycnals are used to better define regimes of the circulation.

2. Method and maps

Potential vorticity was computed from the global dataset prepared by Levitus (1982) from historic NODC data. Levitus supplied annual means of temperature and salinity at 33 standard depths on a 1° grid. The objective analysis used in preparing the data involved smoothing over approximately 700 km. This dataset has the advantages of containing all hydrographic data collected prior to 1978 and resident at NODC and of being a laterally smoothed version of the temperature and salinity fields. A smoothed field is appropriate for analysis of the general circulation except in regions of strong currents and in the surface mixed layer. Levitus' data were used in Keffer's (1985) analysis of the potential vorticity of the world oceans and in an application of Luyten et al.'s (1983) model of thermocline ventilation to the North Pacific (Talley, 1985).

The method for computing potential vorticity is described in Talley and McCartney (1982). Levitus' data were interpolated to 10-meter intervals using a cubic spline followed by linear interpolation to standard density (σ_n) levels separated by 0.05, 0.02 or $0.01\sigma_n$ where n refers to the reference level density. Reference levels of 0, 1000, 2000, 3000 and 4000 db were used. Potential density was calculated using the 1980 equation of state. The in situ density difference between standard density levels was then computed by referencing the in situ temperature and salinity at the density levels to the midpoint. Potential vorticity, $\rho^{-1}f\Delta\rho/\Delta z$, also referred to as Q in the text, was then computed from this density difference and the distance, Δz, between standard density levels. This method is identical to computing the Brunt–Väisälä frequency, N^2, over a given interval Δz and multiplying by $(-f/g)$. The use of potential density surfaces and this particular method of calculating potential vorticity are justified because of the relative flatness of isopycnals in the North Pacific.

It is reasonable to ask whether these maps and sections of potential vorticity computed from averaged hydrographic data represent the "true" ocean. Most major features discussed in this paper were confirmed to occur on synoptic sections (not shown), but mapping was facilitated by using the Levitus data; moreover, the smoothed, averaged fields thus produced are more representative of the large-scale circulation than unsmoothed, synoptic sections.

A large number of vertical sections and maps are presented to give a three-dimensional picture of the North Pacific's potential vorticity. Focal points are isopycnals which outcrop in the North Pacific, isopycnals just below this "ventilated" layer where the circulation is predominantly wind driven, and higher densities where the separation between wind-driven and global thermohaline circulation is not as clear. For comparison with theoretical predictions of the potential vorticity distribution, I have also attempted to find areas of isopycnals where potential vorticity is relatively uniform, where it decreases to the north, where it is dominated by the planetary β effect, and where it increases to the north more quickly than β.

Meridional sections of potential vorticity are shown in Fig. 1; values every 1° along the sections were used. To put them in the context of more familiar quantities, sections of salinity and depth along 160°E are shown in Fig. 2. (Barkley, 1968, presents a large number of such sections in his North Pacific atlas.) Zonal sections of potential vorticity are shown in Fig. 3 using data with 1° longitudinal resolution. The vertical axis on all sections is potential density, σ_θ, and all are displayed so as to emphasize the shallow isopycnals where a density reference level at 0 db is reasonable. Maps of po-

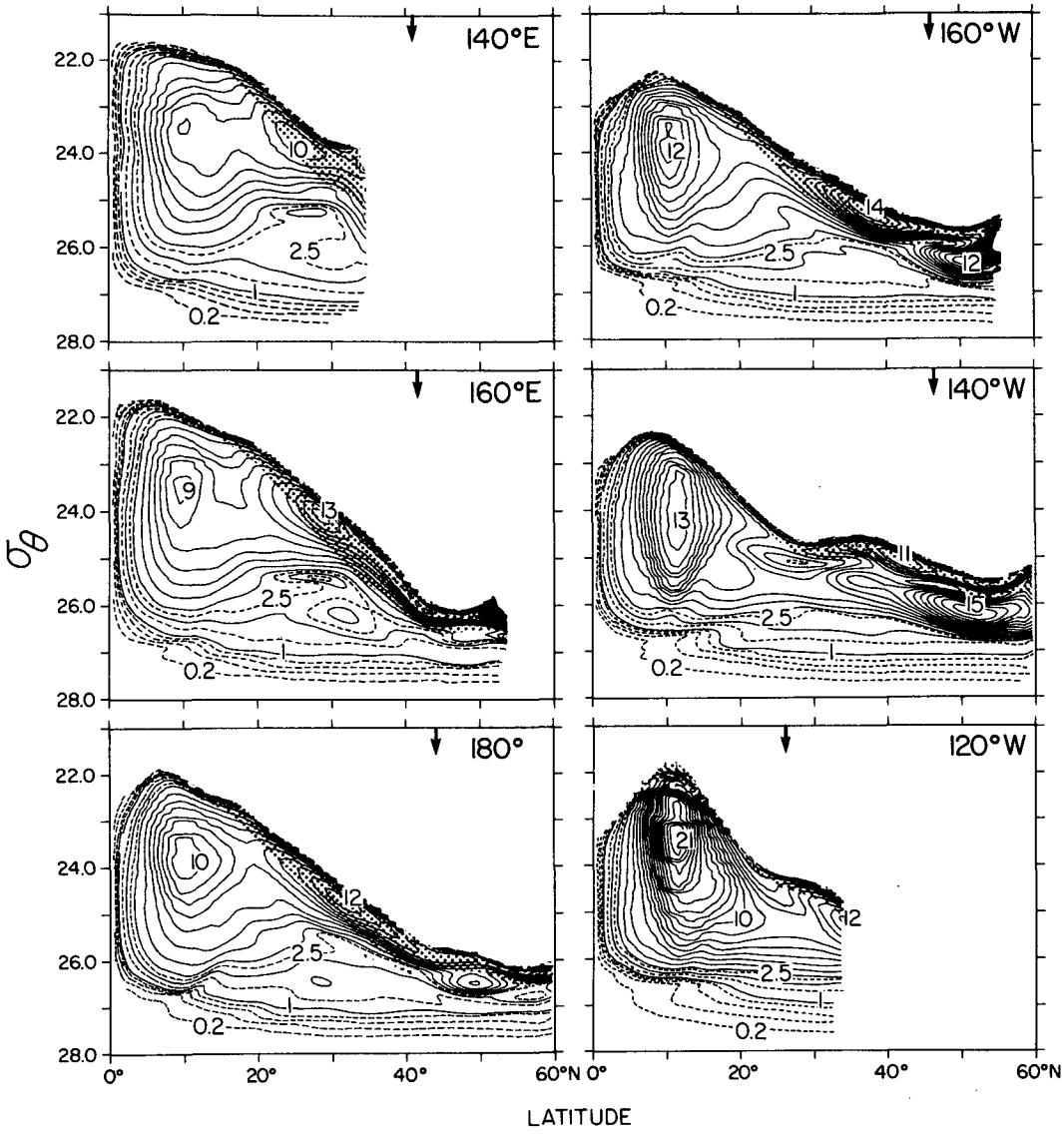

FIG. 1. Meridional sections of potential vorticity as a function of potential density, σ_θ, in the North Pacific. Stepped contours in the tropics arise from the computer contouring routine. Units are 10^{-12} cm^{-1} s^{-1}. The bottom of the shaded area is the winter sea surface outcrop. Arrows indicate the zero of Sverdrup transport.

tential vorticity on isopycnals referenced to 0, 1000, 2000 and 3000 db are shown in Fig. 4, based on a 1° latitude by 5° longitude grid.

Discussion of the sections and maps proceeds from the tropics to the subarctic and from low to high density; subsections deal with the tropics, the ventilated subtropical and subpolar gyres, the top of the unventilated subtropical gyre, and the unventilated subtropical and subpolar gyres.

3. Regimes

a. Seasonal pycnocline

No attempt is made to study the seasonal cycle in detail in this paper. Nevertheless, there are some features of interest north of the average winter outcrop for a given isopycnal, in the regions where water of that density is present only in the warmer part of the year. These regions are shaded in Figs. 1, 3 and 4.

On isopycnals which outcrop in the subtropical gyre, there is a noticeable potential vorticity maximum in the shaded band north of the winter outcrop. The maximum moves out and around the Kuroshio Extension with increasing density. First note the closed 12×10^{-12} cm^{-1} s^{-1} contour in the west at 24.0σ_θ in Fig. 4. As density increses to 25.4σ_θ, this patch moves eastward to 165°W, going no farther than the easternmost extent of the Kuroshio Extension which it parallels. At 25.6σ_θ, the winter outcrop enters the subpolar gyre and the patch of high potential vorticity retreats

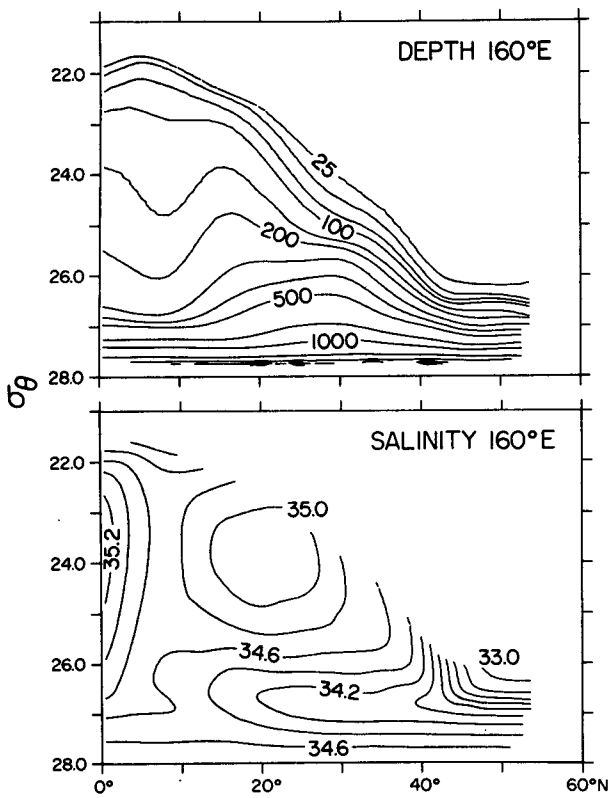

FIG. 2. Meridional sections of (a) depth and (b) salinity at 160°E as a function of potential density, σ_θ.

back to the western boundary with increasing density. Comparison with Reid's (1969) maps of surface density in summer and winter shows that the patches of high potential vorticity occur exclusively where the winter–summer density differences are greater than $2.0\sigma_\theta$. This broad region is centered at the Kuroshio Extension and corresponds to the region of highest annual mean heat loss in the North Pacific. Summer warming aided by advection of warm waters in the Kuroshio Extension creates a summer layer of higher stratification and potential vorticity in the west compared with the east. Reid (1969) also shows that winter surface density is highest in the west and summer surface density is highest in the east; the transition from winter conditions to summer conditions combined with the underlying shape of the gyre (with isopycnals rising from west to east) may produce the observed patches of high potential vorticity and may be implicated in creating a low potential vorticity patch in the eastern Pacific (discussed next).

In the eastern part of the subtropical gyre, represented by the first three isopycnal surfaces in Fig. 4, the seasonal layer has relatively low potential vorticity. It is argued in a later section that the area of exceptionally low potential vorticity, which does not migrate with density, is associated with maximum Ekman pumping. However, the generally low potential vorticity in the outcropping regions in the eastern subtropical gyre may also arise from southward Ekman advection of surface waters, bringing denser water south and weakening the stratification. This contrasts with the situation farther west where Ekman advection may be interrupted by the Kuroshio Extension.

The seasonal pycnocline of the subpolar gyre does not provide much of interest, at least at the resolution of the maps shown here. It consists of very high potential vorticity north and west of the winter outcrop. A much more interesting feature of the subpolar gyre is the low potential vorticity found at and just east of the winter outcrop, to be discussed later.

b. Tropics (0°–20°N)

The tropics are dominated by a cell of high potential vorticity located at approximately 10°N, between the North Equatorial Current and North Equatorial Countercurrent (Figs. 1 and 4). Highest potential vorticity is found between the sea surface and $26.0\sigma_\theta$, covering only the upper 250 m, and is additionally characterized by relatively low salinity and oxygen (Fig. 2b and Tsuchiya, 1968). Potential vorticity is highest in the east where it is greater than 20×10^{-12} cm^{-1} s^{-1} at 120°W. Maps of potential vorticity at 24.0 to $26.0\sigma_\theta$ also show that the tongue of high potential vorticity is most intense near the eastern boundary, with highest values in an isolated patch centered at 130°W. The tongue lies in a band where the mean Ekman vertical velocity is positive, just north of the Intertropical Convergence Zone (Wyrtki and Meyers, 1976; Gill, 1982). Because the band of positive Ekman pumping is so narrow, only the strongest upwelling appeared on a previously published map of Ekman pumping (Talley, 1985), based on winds from Han and Lee (1981). The strongest Ekman upwelling is centered at 130°W and overlies the patch of highest potential vorticity at $24.0\sigma_\theta$.

The tongue of high potential vorticity was apparent but broken in Keffer's (1985) map for the 26.05–$26.25\sigma_\theta$ layer. The tongue was thought to be related to the eastern shadow zone of Luyten et al.'s (1983) model of wind-driven circulation, in which an unventilated region around the eastern and southern sides of the subtropical gyre is predicted. Cox and Bryan (1984) found such a region in a primitive equation model of the North Atlantic and, moreover, found high potential vorticity in the shadow zone even though their model did not contain upwelling in the tropics or along the eastern boundary of the subtropical gyre. The eastern shadow zone in Luyten et al.'s (1983) model as applied to the North Pacific, however, is extremely narrow because the upper water column of the North Pacific is highly stratified (Talley, 1985); hence it is unlikely that the observed wide tongue of high potential vorticity is due entirely to the shadow zone. The correlation between Ekman upwelling along the eastern boundary

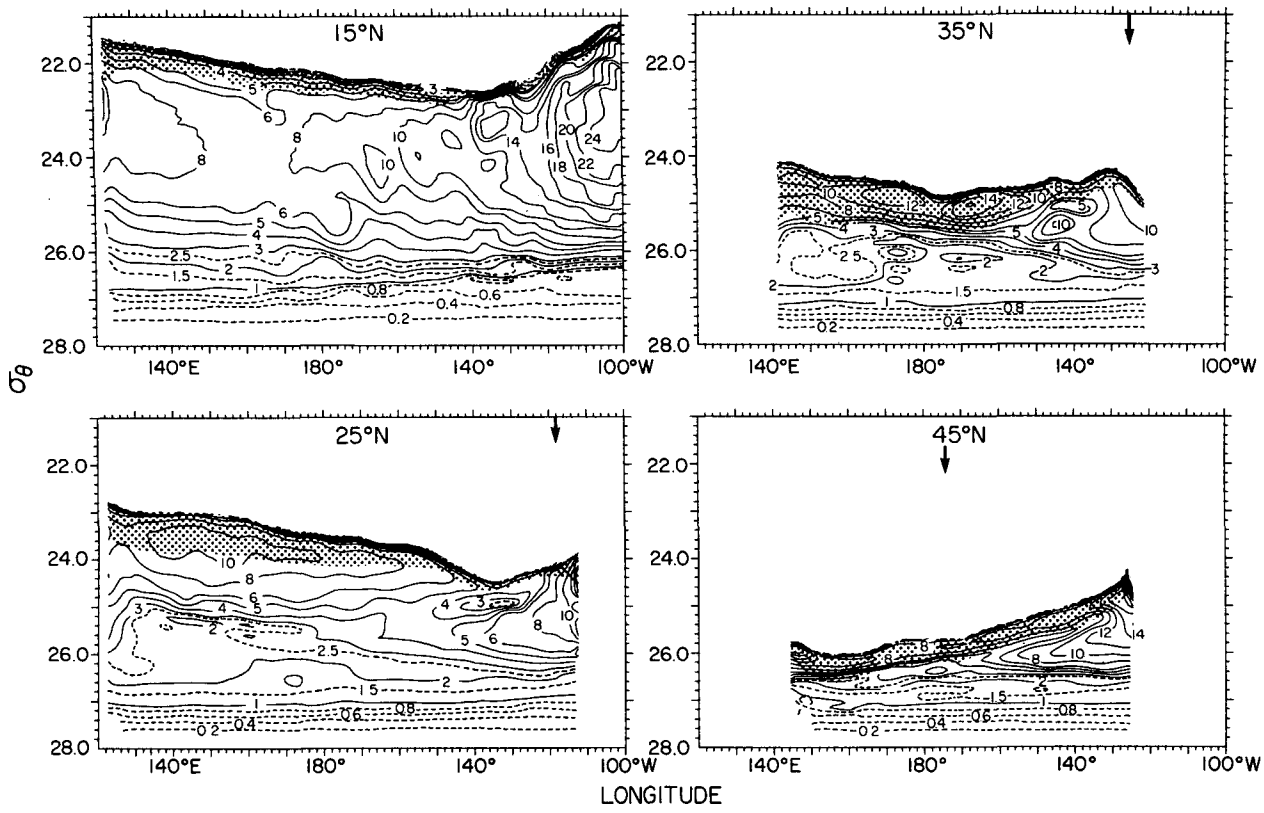

FIG. 3. Zonal sections of potential vorticity in the North Pacific. Units are 10^{-12} cm^{-1} s^{-1}. Arrows indicate the zero of Sverdrup transport.

and 10°N with highest potential vorticity suggests that the highest potential vorticity lies outside the perimeter of the subtropical gyre; it thus arises from a combination of a general increase in potential vorticity eastward and southward in the ventilated subtropical gyre, a narrow eastern shadow zone, and Ekman upwelling outside the subtropical gyre.

Within and just beneath the cell of high potential vorticity, the vertical (diapycnal) gradient of potential vorticity, $\partial Q/\partial\sigma_\theta$, is very high; this can be termed a "vortocline". At higher densities, the gradient is much lower—the transition from high to low vertical gradients is abrupt at all longitudes. On the meridional sections east of 180° in Figure 1, there is a slight minimum in potential vorticity just below the cell of high gradients; this corresponds to a region of slightly lower potential vorticity in the southeast on the $26.6\sigma_\theta$ isopycnal in Fig. 4. The minimum is most pronounced where the overlying high potential vorticity core attains is greatest strength and may arise from exaggerated upward doming of the overlying waters. A similar feature will be noted in the subpolar gyre.

There is no potential vorticity extremum marking the salinity minimum of the Antarctic Intermediate Water which occurs at densities greater than $27.2\sigma_\theta$ and south of 10°N across the entire North Pacific. However, it will be seen in section 3e that Antarctic Intermediate Water and denser waters are distinguished from the overlying waters by the meridional gradient of potential vorticity.

c. *Ventilated circulation: 15°–60°N*

The ventilated isopycnals of the subtropical and subpolar gyres are defined here as those which outcrop at the sea surface in winter. Only portions of the outcropping isopycnals in either gyre are directly ventilated in the sense that flow is directly connected to an outcrop region, but all areas of these isopycnals are described in this section. Neither the ventilation mechanism by which renewed water enters the geostrophic circulation from the mixed layer nor the relative proportion of renewed water in the ventilated regions are the primary issue here. It will be seen that variation in potential vorticity can be related to the extent of ventilation using recent models.

For this paper, the division between the subtropical and subpolar gyres is defined to be the zero of barotropic, wind-driven transport, which is the zero of the zonal integral of Ekman pumping. The vertically integrated (barotropic) streamfunction in a Sverdrup model of the circulation is

$$\Psi = \int_{z_b}^{0} \psi dz' = -\frac{f}{\beta}\int_{x}^{x_E} w_E dx'$$

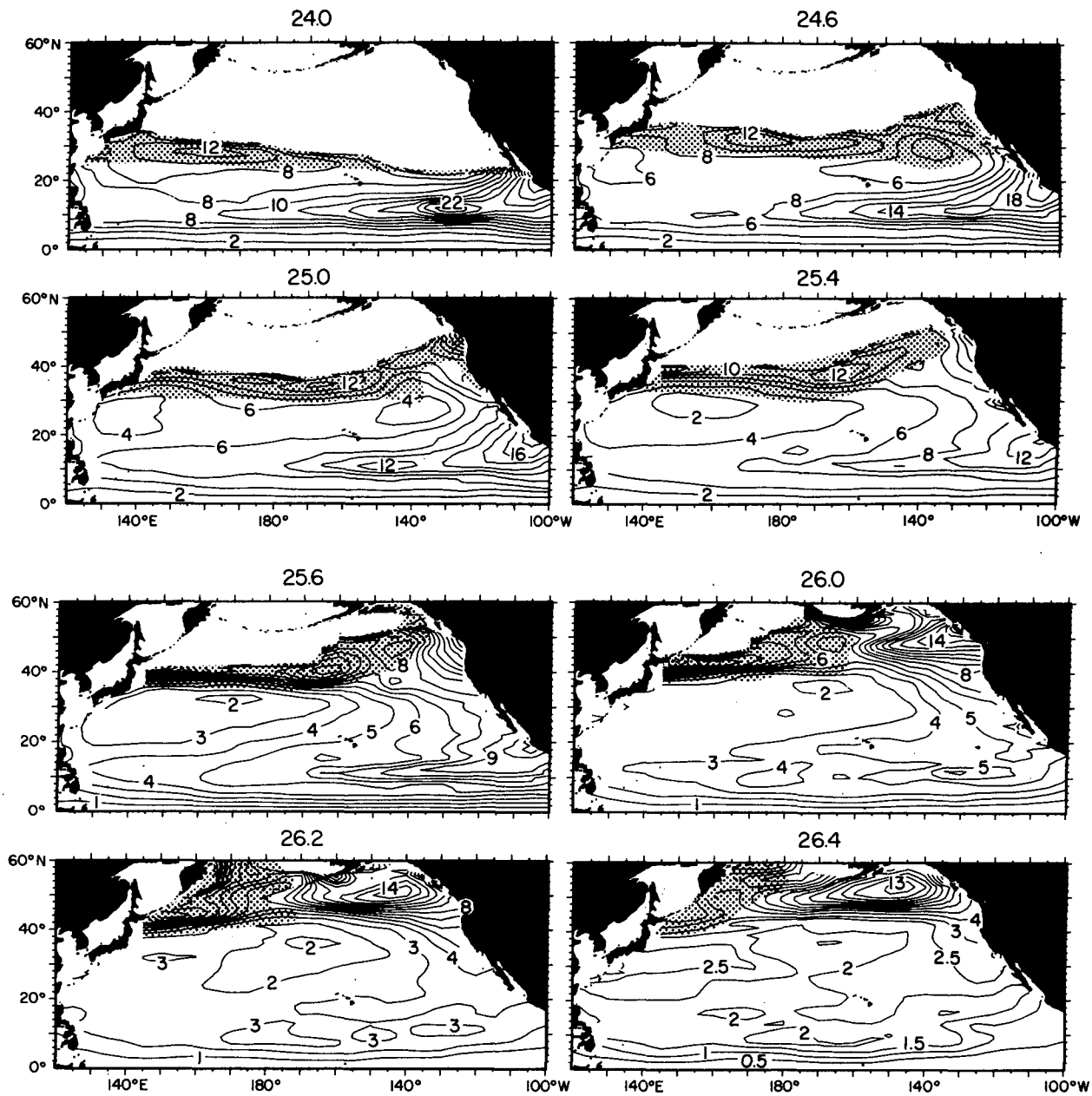

FIG. 4. Maps of potential vorticity on selected isopycnals σ_θ, σ_1, σ_2 and σ_3. Units are 10^{-12} cm^{-1} s^{-1}. Shaded regions are seasonal; their southern edge is the winter sea-surface outcrop.

where z_b is a deep level where the vertical velocity is assumed to vanish, Ψ is the streamfunction, w_E is the Ekman pumping, x_E is the eastern boundary, and f and β are the usual Coriolis parameter and its meridional variation. Clearly there can be no net flow across a contour of constant Ψ and in particular no barotropic flow across $\Psi = 0$ as long as there is a deep level where w vanishes. A map of Ψ based on Han and Lee's (1981) winds is shown in Fig. 5b; because of nonzonality in the Ekman pumping pattern, the zero of Ψ does not coincide with the zero of w_E (Talley, 1985). The zero of Ψ is assumed to define the gyre boundary in subsequent sections; features in the potential vorticity field correspond more directly with this gyre boundary than with the zero of w_E, the Ekman pumping.

The first subsection concerns isopycnals which outcrop south of the gyre boundary, and thus in the subtropical gyre. Isopycnals which outcrop in the subpolar gyre are discussed in the second subsection. Isopycnals which outcrop in both gyres are discussed in both subsections. The third subsection concerns the subtropical portion of isopycnals which outcrop only in the sub-

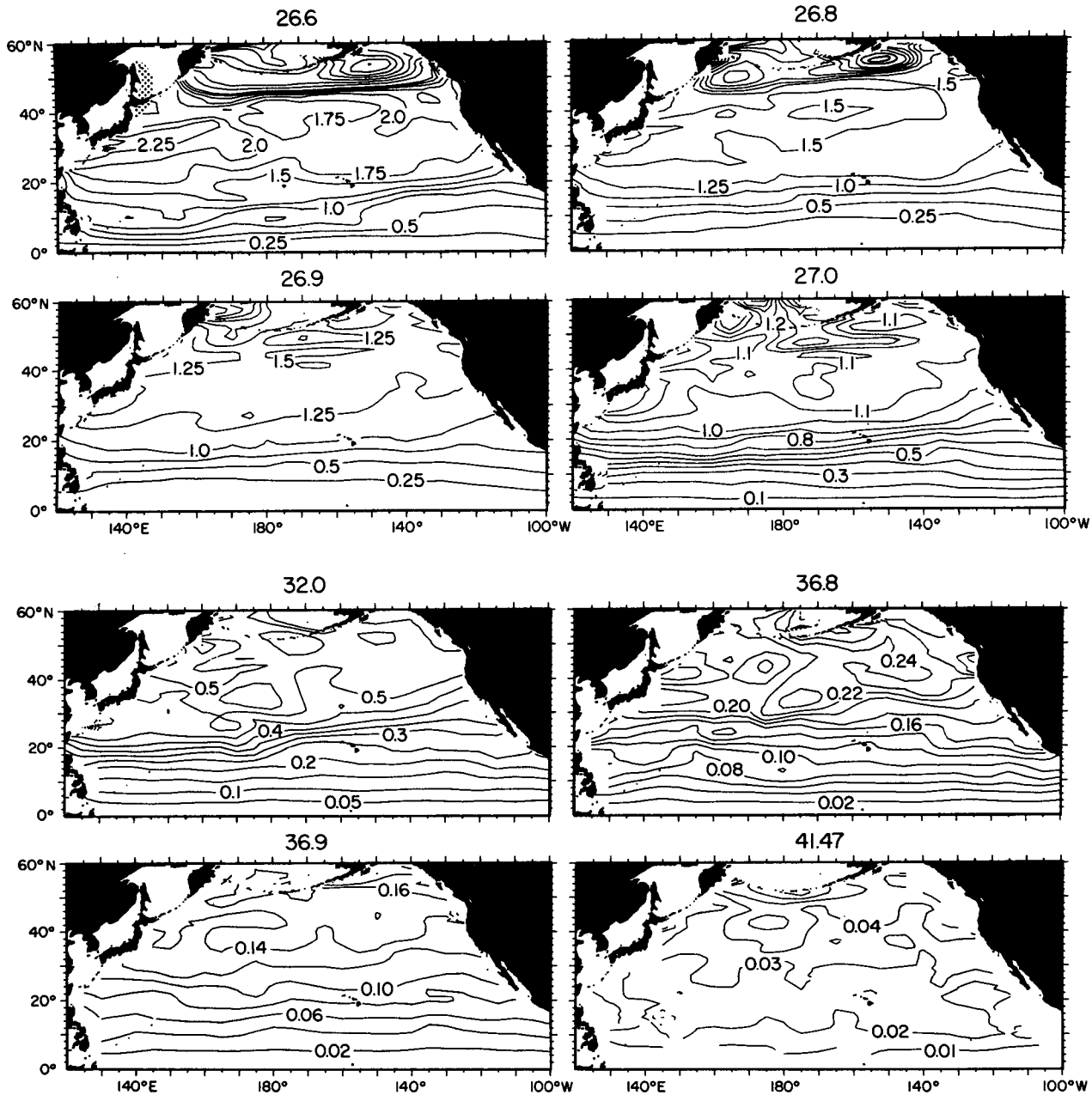

FIG. 4. (*Continued*)

polar gyre and which therefore are unventilated in the subtropical gyre.

1) SUBTROPICAL GYRE (23.0–26.2σ_θ)

Based on maps of average winter sea surface density and the zonal integral of average Ekman pumping (Fig. 5), the highest density which outcrops in the subtropical gyre is about 26.2 to 26.3σ_θ (Talley, 1985). Because of errors in these maps and interannual fluctuations, this density could be higher. However, hydrographic and CTD observations along 152°W in the subtropical gyre in May 1984 show a significant change in water properties at about this density, indicating different processes operating at lower and higher densities (Talley and deSzoeke, 1986). Coats (1981) found a shift to relatively uniform potential vorticity below 26.3σ_θ. For the purposes of this section, 26.2σ_θ is chosen as the bottom of the ventilated subtropical gyre.

We can attempt to distinguish five regimes on isopycnals which outcrop in the subtropical gyre: the seasonal (nonwinter) surface layer, the winter surface layer, a ventilated region where flowpaths originate in the

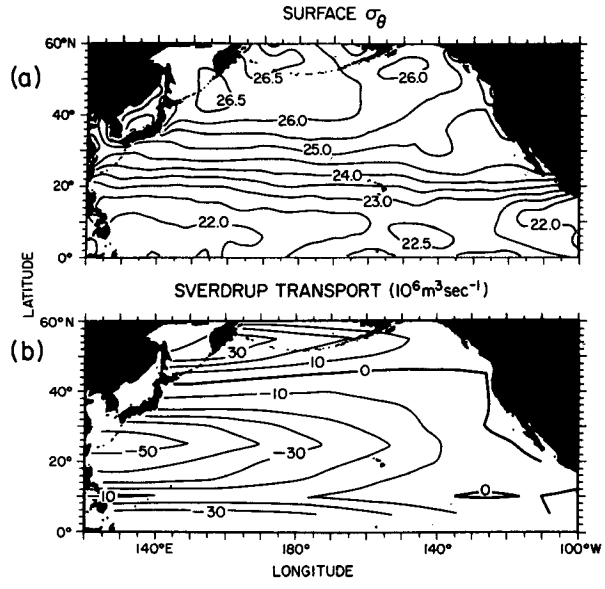

FIG. 5. (a) Sea-surface density in winter, from Levitus (1982). (b) Sverdrup transport function, based on Ekman pumping w_E calculated from Han and Lee's (1981) wind-stress analysis (Talley, 1985).

winter mixed layer and are "subducted" beneath less dense waters to the south, a region ventilated by thermohaline convection (the subtropical mode water of the western part of the subtropical gyre), and a region which is not ventilated in any manner.

The seasonal pycnocline was discussed previously. The dominant feature is a lateral and vertical maximum in potential vorticity which occurs in the region of maximum difference in winter and summer sea surface densities. The maximum potential vorticity moves eastward with increasing density, rounds the end of the Kuroshio Extension region at 165°W, and retreats westward north of the Extension.

Just below the seasonal pycnocline is the wintertime surface layer, which is somewhat difficult to define within the scope of this paper since winter mixed-layer depths are not shown. However, the density of the winter "surface" layer ranges from the winter sea surface density (Fig. 5a) to a somewhat higher density lying at about 100 to 150 meters, based on Reid's (1982) mixed-layer map. The dominant, perhaps unusual, feature of this layer is a lateral minimum in potential vorticity in the eastern Pacific, centered at about 30°N, 140°W, underlying the region of maximum Ekman downwelling. Net surface heat flux in this region is low and uninteresting. From the meridional sections at 25°N and 140°W (Figs. 1 and 2), the density of the vertical minimum is 24.8 to 25.2σ_θ. The lateral minimum is obvious on the maps at 24.6 and 25.0σ_θ (Fig. 4). The region of closed contours enlarges with increasing density, merges with a second low potential vorticity region in the west (the subtropical mode water) and disappears at 25.4σ_θ. The isopycnal depths are not shown but it was found that the lateral and vertical minimum lies in the upper 150 meters of the water column; hence the minimum reflects slightly greater winter mixed-layer depths and possibly excess depression of isopycnals just below the mixed layer.

The lateral potential vorticity minimum is embedded in a corridor of low potential vorticity which lies between the highs of the seasonal pycnocline and the tropics at densities 24.0σ_θ to 25.2σ_θ. It is reasonable to suppose that this zonally elongated region of low potential vorticity is ventilated in the east where potential vorticity is lowest. Note that isopycnals with the low potential vorticity signature outcrop largely south of the maximum in Sverdrup transport (Fig. 5b), in the southern half of the subtropical gyre. Corroboration of ventilation in the low potential vorticity corridor is found in tritium patterns in the upper subtropical gyre (Fine et al., 1981). At 23.9σ_θ a tongue of high tritium extends westward at about the same location as the low potential vorticity feature: it is clear from the location of winter outcrops, sea-surface tritium values, and the existence of a subsurface tritium maximum that the high tritium is due to southwestward advection of ventilated surface waters.

A similar corridor of low potential vorticity is found in the shallow layers of Cox and Bryan's (1984) primitive equation model which is driven by zonally uniform winds and buoyancy fluxes. Pedlosky et al. (1984) showed analytically that low potential vorticity can arise from variations of the isopycnal outcrop latitude which is determined by a coupled mixed layer/ventilated thermocline model with surface heating. In support of their model, low potential vorticity in the North Pacific occurs *only* on isopycnals which outcrop in the southern half of the gyre and whose outcrops appear to be advected somewhat southward in the eastern Pacific. Thus, both the numerical model and analytical theory predict a band of low potential vorticity; a remaining mystery is the apparent coincidence of high Ekman pumping and closed contours surrounding the lowest potential vorticity feature, perhaps indicating the importance of dissipation.

A second low potential vorticity region is evident in the western subtropical gyre at densities greater than 24.8σ_θ, as mentioned before. The eastern and western patches of low potential vorticity merge at 25.2σ_θ (not shown) and the eastern patch disappears at 25.4σ_θ. At 25.4σ_θ, the low potential vorticity in the western Pacific is a vertical and lateral minimum: this is the subtropical mode water (Masuzawa, 1969), a recognizably thick layer of water at about 16°C. As noted by Masuzawa, the pycnostads identified as subtropical mode water (STMW) occur at progressively higher densities to the east. Near the western boundary (140°E in Fig. 1), the vertical minimum in potential vorticity lies at about 25.2σ_θ. In Fig. 4 the patch of potential vorticity less than 2×10^{-12} cm^{-1} s^{-1}, roughly marking the STMW, migrates to the east with increasing density, reaching

a maximum density of about $26.0\sigma_\theta$ and eastward extent to 170°W.

The strongest STMW is located just south of the Kuroshio Extension, in the dynamical center of the subtropical gyre. Application of the Luyten et al., (1983) model of wind-driven subduction to the North Pacific (Talley, 1985) indicates that this region should be unventilated and should have low potential vorticity relative to the ventilated band which surrounds it. However, this is also the region of largest heat loss in the North Pacific, where warm waters advected northward by the western boundary current are cooled: hence ventilation of the region can occur through a mechanism such as wintertime convection, which further decreases the potential vorticity of STMW, as recently modeled by Dewar (1986). Indeed, it is clear from detailed studies of STMW and of the equivalent 18° water in the North Atlantic that winter convection is very active: STMW is marked by an oxygen maximum as well as a potential vorticity minimum (Hanawa, personal communication; Talley and Raymer, 1982). Convective formation of STMW probably occurs just south of the Kuroshio Extension; lateral advection then actively spreads STMW to the south and diffusion increases its potential vorticity. (Lateral smoothing in the Levitus dataset produces the most unsatisfactory results in the neighborhood of strong currents such as the Kuroshio Extension: the correspondence between patches of low potential vorticity and surface outcrops is somewhat marred in the maps and sections shown here. Synoptic winter data show STMW outcropping directly south of the Kuroshio Extension.)

The distinction between ventilation in the western and in the eastern subtropical gyre is the relative strength of wind-stirring and convection in determining winter mixed-layer characteristics. In ventilation by broad-scale subduction such as is surmised for the eastern subtropical gyre, one speculates that the winter mixed layer which is formed by cooling and wind stirring is capped off by seasonal warming, thus becoming an entirely geostrophic part of the interior, Sverdrup circulation whence it flows southward beneath overlying, less-dense waters. The net annual heat flux above subducting mixed layers can be either positive or negative: in the eastern part of the North Pacific's subtropical gyre, the heat flux is close to zero and the sign is in doubt.[1] On the other hand, subtropical mode water is formed in an area of large net heat loss and may be influenced heavily by Kuroshio meandering and rings. Its formation is likely to be patchy and chimney-like, reaching to much greater depths than wind stirring, and its "subduction" due to collapse of convective chimneys rather than the gentler mechanism described for broad-scale subduction.

We have seen that low potential vorticity can be identified with subductive ventilation in the eastern Pacific and with convective ventilation in the western Pacific for densities less than $25.2\sigma_\theta$. The potential vorticity signature of ventilation for densities higher than $25.2\sigma_\theta$ is more ambiguous. Winter outcrops at densities greater than about $25.2\sigma_\theta$ cross from the subtropical gyre into the subpolar gyre so that both gyres are ventilated. Low salinity was shown to be symptomatic of subduction in the eastern Pacific at densities of 25.0 to $26.2\sigma_\theta$ in Talley (1985). In that paper, ventilation was presumed to occur in a band between a western region of low potential vorticity and an eastern/southern region of very high potential vorticity (Fig. 4) based on salinity and an application of the Luyten et al. (1983) model. The region of low potential vorticity also has low potential vorticity gradients: it was identified with the unventilated part of the wind-driven subtropical circulation with embedded, convectively ventilated subtropical mode water. The eastern region of high potential vorticity was identified with Ekman upwelling and is at the perimeter of and outside the subtropical gyre. In the region assumed to be ventilated by subduction, potential vorticity increases to the east and to the south.

The upper horizon of the low-gradient region is $25.0\sigma_\theta$: this is approximately the sea-surface density in winter in the central subtropical gyre where the Sverdrup forcing is maximum (Fig. 5b) and where Sverdrup flow in the surface layers is due southward. The density at the top of the low-gradient region increases to the east, to $26.0\sigma_\theta$ at 140°W (Fig. 3). To the north, the top of the region also slopes gently to higher density, paralleling the sea surface density (Fig. 1). The northern side of the low-gradient region lies at about 40°N in the west and at 46°N in the east: the northern edge is roughly the position of the zero of Sverdrup forcing (Fig. 5b), the nominal boundary between the subtropical and subpolar gyres. The region is thickest in σ_θ in the west at 25° and 30°N, but moves to the central Pacific at 35° and 40°N. This skewing is also evident in the wind forcing and the subtropical gyre, both of which slant from southwest to northeast. The southern edge of the low-gradient region lies at roughly 15°N, which is the southern side of the subtropical gyre in dynamic topography (Reid, 1965).

As density increases from 25.2 to $26.2\sigma_\theta$, the western region of low potential vorticity gradients expands to the east, pushing the region of higher gradients farther towards the edge of the subtropical gyre. The broadest spatial extent of the low-gradient region occurs at about $26.2\sigma_\theta$, which is the base of the ventilated portion of the subtropical gyre based on winter sea-surface density. Potential vorticity in the low-gradient region is generally a lateral minimum. (This contrasts with the situation at densities greater than $26.2\sigma_\theta$ where potential

[1] In response to a reviewer's question regarding the possibility of subduction in an area of net heat loss, it may be possible if the winter mixed layer can be capped off and advected beneath the seasonal pycnocline before the next cooling phase begins.

vorticity in the low-gradient region is more amorphous with patchy extrema.)

The low-gradient region was previously reported by Keffer (1985), Talley (1985), and Rhines (1986) and is evident in Cox and Bryan's (1984) primitive equation model of the wind-driven circulation. It has been identified as the unventilated portion of the wind-driven circulation on isopycnals which outcrop elsewhere in the subtropical gyre and which are ventilated in a band around the low-gradient region (Talley, 1985). (As remarked already, much of the "unventilated" region is actually ventilated convectively just south of the Kuroshio Extension where STMW forms.) As remarked in the previous paragraph, the low-gradient region occurs only on isopycnals which outcrop north of the center of the subtropical gyre. According to crude theoretical notions, all regions of less dense isopycnals, which outcrop farther south, should be ventilated, while an unventilated, western shadow zone of reduced potential vorticity gradients is only possible for isopycnals which outcrop north of the gyre center, where zonal flow is eastward rather than westward. As expected from theory and corroborated in numerical experiments, the unventilated region is smallest on isopycnals which outcrop just north of the gyre center, increasing to fill the entire subtropical gyre at the maximum density which outcrops (Cox and Bryan, 1984; Talley, 1985).

Are lateral gradients of potential vorticity in the unventilated region really zero? Compared with the gradients in ventilated regions above and around the unventilated pool, gradients are indeed very low. They are clearly nonzero where directly affected by subtropical mode water, which ventilates the densities 25.0 to 25.4σ_θ and produces a lateral and vertical potential vorticity minimum. Close examination of potential vorticity on the 160°E section (Fig. 1) shows that the subtropical mode water melds into a well-defined minimum extending northward into the subpolar gyre at the top of the low-gradient region. Such a feature is found on all meridional sections except in the eastern Pacific at 140°W. There is also a maximum at about 30°N and 26.2σ_θ within the low gradient regions at 140°E, 160°E and 180°, whose source is not understood. The significance of the potential vorticity extrema depends on the unknown size of errors in calculation. Zonally averaged potential vorticity and synoptic, smoothed sections of potential vorticity with known error bounds can aid assessment of the structure of the potential vorticity field in the low-gradient region. The latter is not done in this paper, but zonal averages of potential vorticity are examined in a later section.

2) SUBPOLAR GYRE (25.2–26.8σ_θ)

The subpolar gyre is defined to be north of the zero of Sverdrup transport (Fig. 5b). This boundary slopes gently from about 42°N in the west to 45°N in the east. Maximum Ekman upwelling occurs in two separated patches centered at 50°N, 165°E and 55°N, 145°W (Talley, 1985). Average sea surface density in winter ranges from 25.0σ_θ in the east to 26.6σ_θ in the west, excluding fresh coastal currents along the eastern boundary. The isopycnals 25.0 to 26.2σ_θ outcrop in both the subtropical and subpolar gyres. The subpolar circulation in the upper ocean is obviously cyclonic. The bend of the Aleutian Islands and the small north–south extent of the subpolar gyre cause the gyre to be zonally elongated and pinched in the center. Some analyses suggest several cyclonic gyres (Dodimead et al., 1963) but other dynamic topographies indicate a single gyre (Reid, 1965). Potential vorticity will be shown to differ from west to east in the subpolar gyre, but the question of the number of gyres is not resolved.

Potential vorticity on isopycnals which outcrop in the subpolar gyre has a distinctive pattern of high potential vorticity in the eastern Pacific, a band of low potential vorticity near the average position of the winter outcrop, and high potential vorticity west of the outcrop in the seasonal layer. This is illustrated on the isopycnals 25.6 to 26.6σ_θ in Fig. 4 and on the zonal section at 45°N in Fig. 3. This situation closely parallels that of the North Atlantic where waters of low potential vorticity in the region of the winter outcrops have been called Subpolar Mode Water (McCartney and Talley, 1982). Low potential vorticity in the region of the outcrops is due to thickened mixed layers in winter. Because there is a strong, shallow halocline in the subpolar North Pacific, winter mixed layers are constrained to be much thinner than in the North Atlantic; nevertheless, the patterns in the two oceans are strikingly similar. (The maximum mixed-layer depth in the North Pacific is on the order of 100 to 150 meters; using dissolved oxygen saturation as a measure of mixed-layer depth, Reid, 1982, found only one station, in the northwest Pacific, with a winter mixed-layer depth as great as 200 meters. In the North Atlantic, mixed-layer depths can be as large as 500 to 700 meters in the eastern subpolar region and 1500 meters in the Labrador Sea.)

East of the strip of low potential vorticity on outcropping isopycnals is a region of very high potential vorticity. On the shallowest isopycnals, which outcrop farthest to the east, the high potential vorticity abuts the eastern boundary (σ_θ of 25.4 to 26.0). Slightly deeper, on isopycnals which outcrop in the central and western subpolar gyre, there is an isolated patch of high potential vorticity in the east, beneath the maximum Ekman upwelling. The high patch is well defined on meridional sections east of 180° (Fig. 1) and at 45°N (Fig. 3). The area and density range where highest potential vorticity is found correspond closely with the strong halocline of the eastern subpolar gyre. The halocline and high potential vorticity region extend from the base of the winter mixed layer down to about 26.6σ_θ, with a weaker halocline below 26.6σ_θ. In the western subpolar gyre, the density of the winter mixed

layer is 26.5 to 26.6σ_θ over a very large area and only the weaker halocline below 26.6σ_θ is found.

The patch of high potential vorticity resembles the tropical tongue of high potential vorticity which also appears to emanate from the eastern boundary. The tropical feature was identified with Ekman upwelling along the eastern boundary and north of the ITCZ at 10°N; hence the empirical link between high potential vorticity in the eastern subpolar gyre, eastern subtropics, and tropics is Ekman suction. (However, Ekman suction in the subpolar gyre does not completely overwhelm the winter mixed layer which creates low potential vorticity in outcropped areas of isopycnals overlying the dome of high potential vorticity.) If potential vorticity is conserved along streamlines, then streamlines in the region of high potential vorticity in the eastern subpolar gyre cannot connect with the outcrop area where potential vorticity is low on isopycnals. On the other hand, the outcrop regions are actively forced, so potential vorticity is not likely to be conserved along flowlines.

3) Transition to deep water in the subtropical gyre (26.2–26.8σ_θ)

The isopycnals 26.2 to 26.8σ_θ outcrop only in the subpolar gyre and are unventilated within the subtropical gyre. All isopycnals in this transition "layer" are contained in Keffer's (1985) layer B for the Pacific Ocean. Do the properties on these isopycnals reflect ventilation north of the zero of Sverdrup transport or are the two gyres strongly separated? That is, is there baroclinic transport or vigorous mixing between the gyres or are they well separated? Maps of potential vorticity at these densities (Fig. 4) show the large gradient in potential vorticity between the gyres across most of the ocean which was noted by Keffer (1985). Also as noted by Keffer, the meridional gradient weakens near the eastern boundary where relatively high potential vorticity has a tendency to wrap southward along the boundary at 26.2 and 26.4σ_θ. Elsewhere the meridional gradient is reduced only where there is a channel of low potential vorticity in the subpolar gyre, which we have already associated with outcropping; this feature is only apparent with the increased vertical resolution used here. The band of high gradients appears to shift slightly northwards with increasing density and disappears rather abruptly below 26.8σ_θ. Within the subtropical gyre, gradients of potential vorticity are weak: a distinct pattern is not obvious although there is a tendency toward lower potential vorticity in the central part of the gyre. South of the region of low gradients, the potential vorticity contours are more zonal and the north–south gradient is greater than or equal to β. These patterns in the subtropical gyre were noted by Keffer (1985) and are quantified in a later section.

Strong separation of the subtropical and subpolar gyres in this transition layer is indicated by the strength of the meridional gradients. The meridional gradient is presumably maintained by surface forcing, which creates high potential vorticity in the ventilated subpolar gyre and by the presumably diffusive balance which maintains low, homogenized potential vorticity in the unventilated subtropical gyre. The only location where meridional gradients are markedly weaker is near the eastern boundary; in fact, the zero of Sverdrup transport does not extend to the eastern boundary (Fig. 5b) so the subpolar and subtropical regions should not be separated dynamically there. The northward shift of the large gradient band and its shrinkage around the high potential vorticity patch in the eastern subpolar gyre with increasing density point to a more complicated scenario than a vertical "wall" between the gyres at the zero of Sverdrup transport.

d. Unventilated, wind-driven circulation ($\sigma_\theta > 26.8$)

Circulation at densities greater than 26.8 is "unventilated" in the sense that these isopycnals do not outcrop anywhere in the North Pacific. Potential vorticity at 26.8σ_θ resembles potential vorticity on shallower isopycnals which outcrop only in the western subpolar gyre; this may indicate outcropping at 26.8σ_θ in the northwestern Pacific with strong forcing and diffusion from above in the eastern subpolar Pacific or vertical diffusion throughout the region. In contrast, at 26.9σ_θ, which is the next isopycnal shown, the pattern in the subpolar gyre is dramatically different, being relatively featureless and increasingly zonal with increasing density. It thus appears that 26.7 to 26.8σ_θ marks the bottom of the ventilated region or the top of the unventilated water column. This density range is of interest because it matches the density of the main salinity minimum of the subtropical gyre.

Hypotheses concerning the origin of the main salinity minimum center on whether 26.8σ_θ is directly influenced by surface conditions or whether it always lies below the surface layer and is influenced primarily by vertical diffusion, as argued by Reid (1965). It is clear that this isopycnal does not outcrop regularly; winter mixed layers with densities of 26.5 to 26.6σ_θ are often observed, while a surface density of 26.8σ_θ has never been observed. The lack of observations of outcropping probably indicates that vertical diffusion from the directly overlying and outcropping isopycnals is most important in setting the properties at 26.8σ_θ. Hence the salinity minimum is essentially at the *top* of the unventilated column rather than at the bottom of the ventilated column.

Beneath the shallow, eastern, subpolar cell of high potential vorticity is a slight vertical minimum in potential vorticity, e.g. at 26.8 to 27.0σ_θ on the sections at 45°N, 180°. This minimum is the subpolar continuation of a minimum found at lower densities in the northern subtropical gyre just below the vortocline (high vertical gradients of potential vorticity). The vortocline appears to mark the transition from local ven-

tilation to local nonventilation. The correspondence between the subtropical and subpolar minima is unexplained here: the minimum in the northern subtropical gyre may be the winter mixed layer, which is capped by a highly stratified seasonal pycnocline, while the weak minimum in the subpolar gyre lies below the seasonal pycnocline, winter mixed layer, and strong pycnocline (halocline). The potential vorticity minimum below the subpolar vortocline may result from required compensation for the upward doming and high potential vorticity on overlying isopycnals. It therefore appears that the maximum depth of direct influence of Ekman suction is the bottom of the vortocline. (A similar minimum beneath the very high potential vorticity cell in the eastern tropics was remarked upon earlier.)

The lateral potential vorticity structure below $26.8\sigma_\theta$ in the subpolar gyre becomes amorphous and gradients between the gyres decrease and disappear (Fig. 4), as noted by Keffer (1985). Moving down the water column to σ_1, σ_2, and σ_3 isopycnals, the region of low potential vorticity gradients shrinks northward, with a band of high meridional gradients to the south separating it from a region where the meridional potential vorticity gradient is β-like. The depth of a representative isopycnal ($32.0\sigma_1$) in this set is shown in Fig. 6. Although potential vorticity is nearly uniform over a large area, there are nevertheless large depth excursions related to the subpolar and subtropical circulations; the maximum depth change occurs at the gyre boundary defined by the Sverdrup transport. However, the gyre boundary is transparent to the potential vorticity field, indicating that there is cross-gyre transport or mixing on these wholly unventilated isopycnals, even though there are well-defined subpolar and subtropical gyral circulations. I favor the mixing mechanism because strong evidence for cross-gyre transport was not found at shallower levels where potential vorticity gradients were maintained against mixing by surface sources: on the wholly unventilated isopycnals, there are no strong sources to maintain gradients. On the densest isopycnal shown ($41.47\sigma_3$), which lies at about 2500 meters, the potential vorticity pattern is rather noisy but shows an overall increase northward, which will be seen to be β-like in the next subsection.

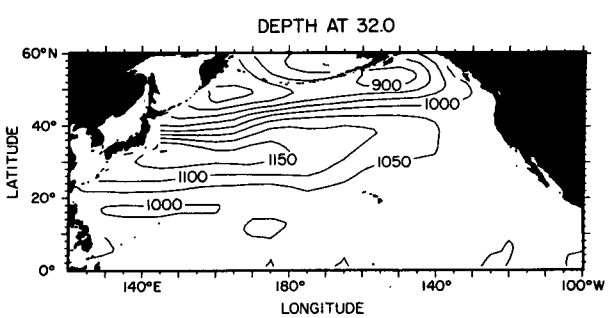

FIG. 6. Depth (meters) of $32.0\sigma_1$.

In summary, well-defined regions of low potential vorticity gradients have been found on unventilated isopycnals to a depth of about 2500 meters. The patterns of potential vorticity are nevertheless noisy; it is not clear whether the gradients are significant or whether potential vorticity is "uniform" in some sense. Because rigorous error analysis is difficult, the question can only be answered qualitatively. The important observation is that there are regions where ∇Q is greatly reduced, where Q is potential vorticity. By zonally averaging potential vorticity, the errors and noise can be reduced. This is done in the next subsection: clear distinctions between regions where $\partial Q/\partial y$ is β-like, where it is greater than β, and where it is essentially zero emerge.

e. Zonally averaged potential vorticity

The maps and vertical sections of potential vorticity presented in the previous section were useful for identifying regions on partially ventilated and wholly unventilated isopycnals with specific regimes predicted by recent theories. Areas of isopycnals which appear to be strongly affected by local surface sources were also obvious, and the necessity for diffusion, both along and across isopycnals, was indicated. Recent theories (e.g., Rhines and Young, 1982; Young and Rhines, 1982; Pedlosky and Young, 1983) suggest that areas of low potential vorticity gradients correspond with regions of unventilated, wind-driven circulation. Regions apparently unaffected by the wind are identified by meridional gradients equal to β: circulation in these areas would be thermohaline or strongly diffusive. Meridional gradients can of course take many values other than zero or β, particularly on ventilated isopycnals where large regions of negative meridional gradients are found. Zonal averages of potential vorticity are more easily compared with the oceanic "rest state" where potential vorticity is proportional to the Coriolis parameter. Zonal averaging also reduces the noise of the maps in Fig. 4.

Zonal averages every 1° of latitude were computed from longitudinal sections separated by 5° and are only shown if there was at least 45° of longitudinal coverage, that is, 10 points in the average; this cutoff was chosen subjectively based on a large increase in noise for smaller numbers of observations. The average potential vorticity is shown in Fig. 7 for isopycnals which represent each of the regimes discussed previously and for a representative group of depths; the figures shown were selected from a much larger group of isopycnal averages. The smooth curve in each figure is the potential vorticity field that would exist if the meridional gradient were entirely due to the variation of the Coriolis parameter, it was calculated by averaging $\rho^{-1}\partial\rho/\partial z$ for the entire isopycnal surface in the North Pacific and

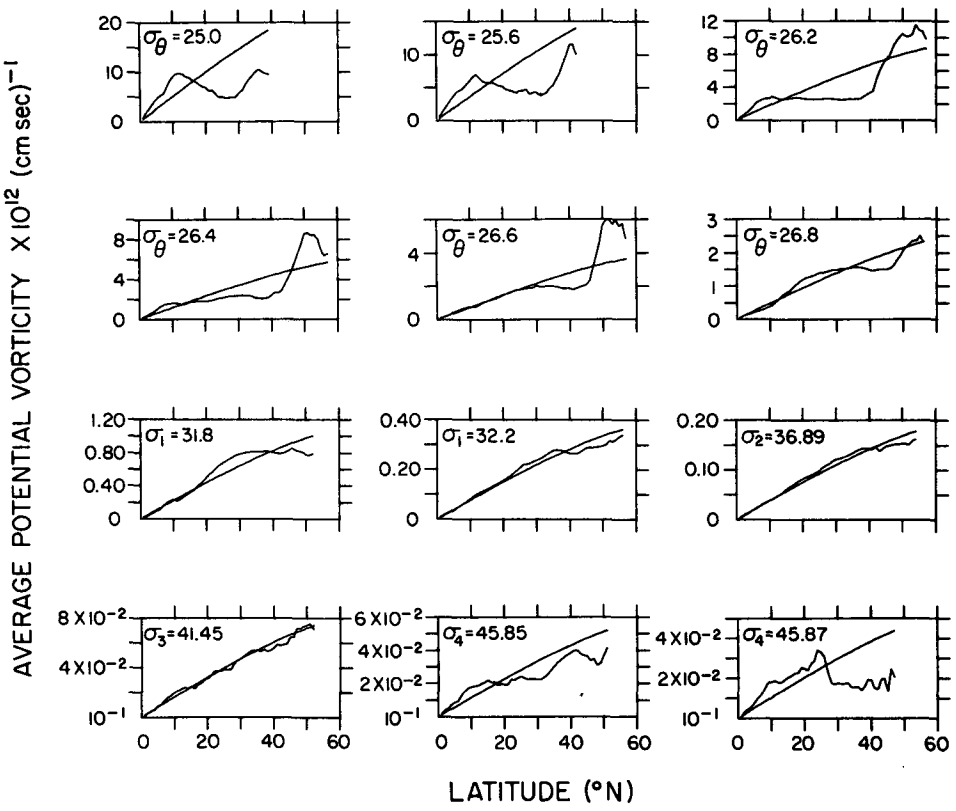

FIG. 7. Zonal average of potential vorticity at selected densities (jagged curves) and $\rho^{-1}f\partial\rho/\partial z$ based on the average of $\partial\rho/\partial z$ over the entire North Pacific for that isopycnal (smooth curves). Values are shown only at latitudes where there was at least 45° of longitudinal coverage, although the underlying smooth curve is based on all available points. Vertical scales vary for each panel.

then multiplying by f. Obviously if the jagged, zonal average of potential vorticity, $\rho^{-1}f\partial\rho/\partial z$, is parallel to the smooth β-curve, the potential vorticity gradient is β.

The different regions of ventilated and unventilated isopycnals discussed in the previous subsections are quite apparent in Fig. 7. There is a striking distinction between regions where $\partial Q/\partial y$ is less than, equal to, or greater than β. On isopycnals which are ventilated in the subtropical gyre (25.0 and 25.6σ_θ), there is a maximum in Q at 10°N which decreases to a minimum value at the southernmost average outcrop latitude. Between the equator and the maximum $\partial Q/\partial y$ is greater than β. The northward decrease in potential vorticity in the southern part of the subtropical gyre is well known and provides fertile ground for baroclinic instability. North of the minimum, which marks the outcrop in the subtropical gyre, potential vorticity increases faster than β to a maximum. Although the 25.0 and 25.6σ_θ isopycnals also outcrop in the subpolar gyre, there was not enough zonal coverage there to be included in the average; the tendency, however, is toward high potential vorticity in the subpolar gyre. The signature of ventilation in the subpolar gyre on the maps in Figure 4 was a band of low potential vorticity; this only weakly influences the zonal averages because of the strongly nonzonal subpolar gyre patterns.

On isopycnals which are ventilated only in the subpolar gyre (26.2 and 26.4σ_θ), Q is markedly uniform in the subtropical gyre with a sudden increase to subpolar values commencing at the southernmost latitude of the sea surface outcrops. The southern edge of the plateau in potential vorticity is again at about 10°N; $\partial Q/\partial y$ south of 10°N is greater than β. The difference between the potential vorticity plateaus on these isopycnals and the northward decrease in potential vorticity on shallower isopycnals is quite striking. There are two strong sources of potential vorticity in the subtropical gyre on the shallower, outcropping isopycnals: the tropical maximum produced by Ekman upwelling and the minimum at the outcrop. When the latter source is missing, potential vorticity must be set by vertical fluxes which control the tropical and subpolar levels. On all four isopycnals (25° to 26.4σ_θ), the gradient between the subtropical and subpolar gyres is very high.

At 26.6 and 26.8σ_θ, there is a transition to the distribution of potential vorticity found at deeper levels. Potential vorticity is dominated by f in the tropics before increasing more quickly and then flattening to start

a plateau. However, surface forcing remains a strong influence in the subpolar gyre so potential vorticity remains high there.

At densities just below $26.8\sigma_\theta$, a plateau in potential vorticity spanning both gyres is apparent, as illustrated at $31.8\sigma_1$. As was seen in the subsection on unventilated isopycnals and in Keffer (1985), the gyre boundary at these densities is transparent to potential vorticity although there is a large change in depth between the gyres and although dynamic calculations distinctly show separate subtropical and subpolar gyres. The latitude band where potential vorticity is nearly uniform shrinks with depth and finally disappears at about $37.0\sigma_2$ ($41.47\sigma_3$); this isopycnal is nearly flat and lies at about 2600 meters.

There is one last regime in the zonal averages of potential vorticity: on isopycnals below 3100 meters, the meridional gradient is less than β, as exemplified by $45.85\sigma_4$. (Potential vorticity was calculated using $0.01\sigma_4$ layers because $0.02\sigma_4$ layers were much too thick in the abyssal waters.) This might indicate either the effect of basin-scale topography or geothermal heating in modifying the effective β in the abyssal waters. North of 30°N, there is a gradual, broad-scale shoaling of the bottom to the east which rotates the contours of f/h for the abyssal layers (and barotropic mode) away from zonality, as shown in Levitus (1982). This should reduce the meridional gradient of the zonally averaged potential vorticity but should tend to increase its overall value. However, potential vorticity at 45.85 and $45.87\sigma_4$ is flattened and decreased, an effect which could be caused by geothermal heating of the deep water. The oldest abyssal water is in the north and has been subjected to the most heating, which should tend to reduce its thickness and potential vorticity (Joyce et al., 1986).

Figure 8 is a schematic diagram of the different regimes of $\partial Q/\partial y$ seen in these zonal averages as a function of depth and density. Regions where $\partial Q/\partial y$ is negative, effectively zero, less than β, β-like, and clearly larger than β are indicated. These figures were produced qualitatively from the zonal averages shown in Fig. 7. Because error bounds were not placed on $\partial Q/\partial y$, it was not possible to be more quantitative, but it is likely that a more rigorous approach would produce much the same figure. Figure 8 clearly shows that the meridional band of potential vorticity which is distorted away from the "rest state" of total domination by f becomes narrower with depth, is centered at the gyre boundary with depth, and disappears entirely at about 2600 meters. "Distortion" in the upper 300 meters follows a general pattern from equator to pole of a band of gradients higher than β, a band of negative gradients, a band of uniform potential vorticity, and a band of high gradients north of which is a "hodgepodge" in the subpolar gyre where zonal averaging does not make sense. The region of negative gradients associated with outcropping disappears directly below this part of the water

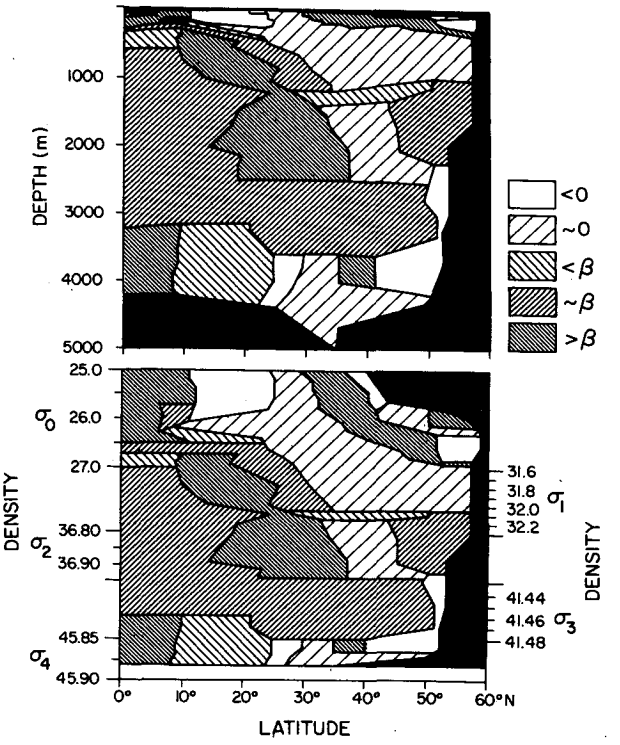

FIG. 8. Regimes of the meridional gradient of potential vorticity $\partial Q/\partial y$, based on zonally averaged potential vorticity as shown in Fig. 7. Black indicates lack of data due to land, sea surface outcrops and unexamined isopycnals at the ocean bottom south of 35°N.

column. Below $26.9\sigma_\theta$, the northern band of high gradients disappears and the uniform potential vorticity extends all the way to the north. Below 1200 meters or $32.0\sigma_1$, a different regime with distortion restricted to central latitudes appears. Between 2600 and 3200 meters, the β-effect dominates the full basin with the exception of a narrow band of negative gradients at the northern boundary. Below 3200 meters, the potential vorticity field is again distorted, particularly north of 20° to 30°N, the latitude of the Hawaiian Islands.

4. Discussion

The potential vorticity distribution on a given isopycnal in the North Pacific strongly depends on whether the isopycnal is ventilated in the subtropical and/or subpolar gyre; if unventilated, its properties are affected by proximity to the sea surface and hence by the presence of strong, direct forcing and by the presence of wind-driven circulation.

On the shallow isopycnals, there is a strong correlation between the potential vorticity field and the strength of Ekman upwelling and downwelling, to such an extent that closed contours of potential vorticity can occur beneath especially strong forcing regions. This occurs in the strongest upwelling regions in the eastern tropics and in the eastern subpolar gyre. High potential vorticity is also found along the eastern

boundary in the subtropics beneath suspected Ekman upwelling where surface heating is the greatest (Talley, 1984). Lowest potential vorticity in the subtropical gyre is found near the sea surface in isolated areas in the east and west. The patch in the east is correlated with strong Ekman downwelling. The patch of low potential vorticity in the west is subtropical mode water (Masuzawa, 1969) and is correlated with the greatest cooling in the North Pacific (Talley, 1984). Undoubtedly both wind-driving and buoyancy flux are important in producing potential vorticity extrema in the surface layers.

Ventilation in the shallow layers which outcrop in the southern subtropical gyre is marked by low potential vorticity. With increasing density, the ventilated region is identified with higher lateral gradients of potential vorticity compared with a western region of low gradients which is identified as unventilated based on recent theories; ventilation is substantiated by tritium analyses (Fine et al., 1981). Potential vorticity increases smoothly eastward across the ventilated region to a maximum near the eastern boundary where the highest potential vorticity is probably associated with Ekman upwelling. The tongue of high potential vorticity found at the eastern boundary encircles the subtropical gyre at shallow depths and extends westward in a tongue in the tropics, also beneath Ekman upwelling. Thus the high potential vorticity probably has a number of sources: Ekman upwelling, ventilation of the subtropical gyre, the "eastern shadow zone" of the Luyten et al. (1983) model, and net surface heating. All four sources may be important and cannot be differentiated among based on the maps presented here.

In the western subtropical Pacific there is a "pool" of low potential vorticity that expands in size with increasing density and encompasses the entire gyre at 26.2 to 26.3σ_θ. Potential vorticity within this region has fairly low horizontal gradients and the region was identified as the unventilated portion of the otherwise ventilated isopycnals. The boundary between "ventilation" and "nonventilation" is not abrupt on any isopycnal, but was roughly identified as a change in lateral gradients. At the top of the pool of low potential vorticity is the subtropical mode water, which is markedly lower in potential vorticity than waters above, below, and around it. The subtropical mode water is ventilated in winter by relatively deep convection rather than by the subtropical ventilation that occurs by wind-driven subduction of the surface mixed layer on a broader scale.

Overall, the distribution of low potential vorticity "water masses" or pycnostads in the subtropical gyre is remarkably like that of the North Atlantic. Both oceans have a subtropical mode water of similar volume, spatial distribution, and density relative to the total range of density found in each ocean. Both oceans also contain water of low potential vorticity in the eastern subtropical gyre, which appears to originate in the northwestern part of the gyre at the sea-surface outcrops. In the North Pacific this feature in its southwestward extension around the subtropical gyre are extremely close to the sea surface; they are not remarkably thick compared with a similar feature in the North Atlantic noted by McCartney (1982), who concluded that this "mode water" was formed in the subpolar gyre and recirculated into the subtropical gyre. The different interpretation presented here may result from a difference in the definition of the gyre boundary.

Ventilation in the subpolar gyre is marked by a strip of water of low potential vorticity (pycnostad) roughly paralleling the curving isopycnal outcrops. This feature is similar to the subpolar mode water (SPMW) of the North Atlantic (McCartney and Talley, 1982) and the Southern Ocean (McCartney, 1977), although the thickness of the pycnostads is much greater in these oceans. Subpolar mode water in other oceans is believed to be formed by winter convection (wind-stirred mixed layers do not penetrate to 400 or 500 meters), but circulates predominantly due to wind driving. Cyclonic circulation in the North Atlantic advects the pycnostads around the subpolar gyre, allowing the pycnostads to be reformed at higher densities in succeeding winters. Since the depth of the winter mixed layer in the North Pacific is limited by a shallow halocline, the pycnostads in the subpolar North Pacific are much thinner than their counterparts in the North Atlantic. Because the subpolar gyre is so meridionally compressed compared to the North Atlantic, and because the basic data used here are spatially smoothed, only a crude outline of the distribution of this North Pacific subpolar mode water is possible; how the circulation and pycnostads mesh is not clear and is the subject of additional study.

The density of SPMW in both the North Pacific and North Atlantic increases around the cyclonic gyre, although the pycnostads in the North Pacific are considerably weaker than those of the North Atlantic. The salinity at the sea surface and of the SPMW increases around the North Pacific gyre rather than decreasing as it does in the North Atlantic. (However, salinity on a given isopycnal decreases around the gyre in the North Pacific.) The North Atlantic and North Pacific also have intermediate-depth salinity minima, the Labrador Sea Water and North Pacific Intermediate Water, respectively. The Labrador Sea Water is the densest form of SPMW in the North Atlantic and is also a strong potential vorticity minimum; in the North Pacific, there is actually a very weak potential vorticity minimum in the subpolar gyre near the density of the North Pacific Intermediate Water. The correspondence of pycnostads in the two oceans ends here: in the Labrador Sea Water, the potential vorticity and salinity minima are nearly coincident geographically throughout the subpolar gyre and in the western subtropical gyre. In contrast, the North Pacific Intermediate Water is found only in the subtropical gyre and appears, at 26.8σ_θ, to be slightly denser than the densest water

commonly found at the sea surface, at $26.6\sigma_\theta$, although this may reflect a simple lack of observations. The weak potential vorticity minimum in the North Pacific is found only in the subpolar gyre, just beneath the very high potential vorticity layer. The two oceans differ as a result of the shallowness of the winter mixed layer in the North Pacific and the presence of high-salinity Mediterranean Water in the North Atlantic. The former precludes the presence of strong (thick) pycnostads and a strong middepth potential vorticity minimum in the North Pacific; the latter precludes a salinity minimum pervading the entire North Atlantic subtropical gyre. In both oceans, the intermediate salinity minimum indicates the maximum density of direct ventilation, but while Labrador Sea Water renewal has been directly observed, North Pacific Intermediate Water has never been observed to outcrop in winter.

It was surmised that the subpolar and subtropical gyres are strongly separated on isopycnals which outcrop in both gyres and on the isopycnals 26.2 to $26.6\sigma_\theta$ which outcrop only in the subpolar gyre, based on large gradients of potential vorticity near the gyre boundary as defined by Sverdrup transport. Within the subtropical gyre at these higher densities, potential vorticity is nearly uniform; in the zonal averages it appears as a remarkable plateau between the tropics and the gyre boundary. North of the subtropical gyre, potential vorticity increases very quickly to a maximum in the central subpolar gyre. The northern edge of the subtropical plateau appears to migrate northward with increasing density.

Gradients of potential vorticity on wholly unventilated isopycnals are low over a large area extending across the apparently transparent gyre boundary. (The gyres may be as strongly separated as at lower densities, but in the absence of direct surface forcing, the potential field is determined by diffusion; apparently isopycnal diffusion dominates over cross-isopycnal diffusion.) The low-gradient area decreases in size with increasing density and depth, is centered at the gyre boundary (hence poleward-intensified with depth in the subtropical gyre) and eventually disappears at about 2500 meters. The low-gradient region extends over the entire longitudinal range of the North Pacific; its southern boundary tilts slightly from southwest to northeast. South of the low-gradient region the potential vorticity field is strongly zonal and potential vorticity increases more rapidly than f; outside this region, potential vorticity is dominated by β. Between 2500 and 3500 meters, the potential vorticity is dominated entirely by β. Below 3500 meters, the meridional profile of potential vorticity is noisy but flattened north of 10°N.

The potential vorticity distribution at depths below 500 meters is consistent with previous analyses of the circulation and with the distribution of properties such as oxygen. Reid and Mantyla's (1978) maps of oxygen at $32.0\sigma_1$ and geopotential anomaly at 1000 db relative to 3500 db indicate an anticyclonic gyre north of 30°N. This circulation lies entirely within the region of homogenized potential vorticity at $32.0\sigma_1$. A separate and weaker anticyclonic circulation south of 30°N is indicated by the geopotential anomaly and oxygen maps: potential vorticity field is dominated here by β and therefore the circulation is presumed to be thermohaline rather than wind driven, based on recent circulation theories. Reid and Arthur (1975) showed conclusive evidence of poleward migration of the subtropical gyre with depth. Their gyre coincides with the region of low potential vorticity gradients which shrinks northward to the gyre boundary with increasing density (Fig. 4).

The potential vorticity observations presented here extend Coats' (1981) observations at (35°N, 155°W) and Keffer's (1985) maps of potential vorticity in the upper North Pacific. Coats found a thick layer from 350 to 1100 meters where lateral potential vorticity gradients were too low for implementation of the β-spiral method; his results correspond to the nearly uniform potential vorticity shown here at 35°N at densities of $26.2\sigma_\theta$ to $32.1\sigma_1$ and over the depth range 300 to 1300 meters. Keffer's potential vorticity maps, computed from the same dataset used here, exposed the most important features of the ventilated subtropical and subpolar layers and of an unventilated layer just below them. These include the tongue of high potential vorticity encircling the subtropical gyre, very high potential vorticity in the eastern subpolar gyre, and a large region of low gradients in the unventilated layer. The present study slices the North Pacific much more finely and extends to abyssal depths: it is encouraging to find that all features shown in Keffer's thicker layers are present. The thinner slices which intersect the sea surface allow identification of low potential vorticity associated with ventilation in both the subtropical and subpolar gyres, show the vertical structure and strength of the high potential vorticity features, and show the increasing size of the low-gradient region in the western subtropical gyre as density increases. Below the ventilated upper layer, the new study shows how the low-gradient region, identified from theory as the unventilated wind-driven circulation, shrinks poleward with increasing density. At abyssal depths, a second region of lower potential vorticity gradients emerges and is tentatively associated with geothermal heating of the deep waters.

One reason for mapping potential vorticity is that it is the fundamental dynamical quantity in theories of large-scale ocean circulation. Although it was not possible to include relative vorticity in the calculations, it was not presumed necessary since relative vorticity is unimportant except in boundary layers in the largest scales of circulation. Four types of models and their offshoots are especially relevant. They are models of the shallow circulation and isopycnal outcrops (e.g., Parsons, 1969; Huang, 1986), models of the ventilated circulation (e.g., Luyten et al., 1983), models of the

wholly unventilated circulation (e.g., Rhines and Young, 1982), and models of the abyssal circulation (e.g., Stommel and Arons, 1962). In addition, recent numerical models fill the gap between observations such as those presented here and highly idealized analytical models (Cox and Bryan, 1984; Cox, 1985).

The models based on Parsons (1969) indicate that isopycnal outcrops in the northern subtropical gyre should cross to the subpolar gyre. Isopycnals outcropping further south should be nearly zonal with a slight northwest-to-southeast tilt due to advection (Pedlosky et al., 1984). The winter sea surface density in the North Pacific (Fig. 5a) shows that, indeed, isopycnals from the northern half of the subtropical gyre curve northward and cross into the subpolar gyre, while outcrops in the southern half of the gyre are nearly zonal. The demarcation between the northern and southern "halves" of the subtropical gyre appears to be where the southward Sverdrup transport is maximum.

Despite the imposition of zonal outcrops throughout the subtropical gyre, the ventilated thermocline models (e.g., Luyten et al., 1983) are remarkably successful in predicting the occurrence of ventilated and unventilated regions. The predictions of a ventilated corridor, an unventilated eastern shadow zone, and an unventilated western shadow zone which increases in size to fill the entire subtropical gyre at the maximum ventilated density are substantiated by observations in the North Atlantic (Luyten et al., 1983), in the North Pacific (Talley, 1985 and here) and in the South Pacific (deSzoeke, 1987). The models predict that the lowest potential vorticity should be found in the western shadow zone, that it should probably have small lateral gradients there, and that potential vorticity should increase away from this shadow zone. A numerical model (Cox and Bryan, 1984) shows that potential vorticity is highest in the eastern shadow zone. Fairly detailed agreement between flow paths predicted by the model based on actual winds and actual flowpaths is also found (Talley, 1985). What these models do not do is produce the observed isolated lows and highs of potential vorticity at locations of strong Ekman pumping and buoyancy flux. They also do not include mixing, which must be important in setting the value of potential vorticity in the unventilated regions and in modifying potential vorticity along flow paths in the ventilated regions.

The circulation of the ventilated layers in the subpolar gyre is not modeled as well as the subtropical circulation. All theories produce the observed cyclonic circulation, but because they do not include buoyancy flux and do not model the subsurface flow well, the potential vorticity distribution presented here, which is similar to that of the North Atlantic, is not reproduced.

Models of wholly unventilated circulation (Rhines and Young, 1982; Young and Rhines, 1982, etc.) successfully predict regions of low lateral potential vorticity gradients. Low *vertical* gradients are also observed in the North Pacific. These models also show steep gradients of potential vorticity south of the region of uniform potential vorticity: a schematic of the potential vorticity distribution arising in a thought experiment (Fig. 8 in Rhines and Young, 1982) is remarkably similar to Fig. 7 here. Young and Rhines (1982) estimated that the depth of wind-driven circulation in the North Pacific should be 2300 meters; this agrees well with the depth of 2500 meters found here. The shape of their predicted gyre is also reasonable; the subtropical gyre shifts poleward and the subpolar gyre shifts equatorward with depth so that at its deepest, the circulation is centered at the gyre boundary. One peculiarity found here is that the meridional width of the gyre appears to jump discretely with depth rather than being as smooth as the theoretical gyre. The tremendous longitudinal extent of the unventilated region is also a surprise: the low gradient region does not appear to shrink to the west as is predicted in unventilated models with realistic wind forcing and western boundary currents (Young and Rhines, 1982).

Outside the wind-driven gyres, circulation must be driven entirely by thermohaline forcing, which can affect circulation in wind-driven regions as well. There is every reason to suppose from dynamic computations that there is circulation in regions where potential vorticity contours are approximately zonal. The Stommel and Arons (1960) model predicts a potential vorticity distribution dominated entirely by f with poleward flow driven by internal upwelling. It is clear from published analyses of intermediate and deep circulation in the North Pacific (Reid, 1965) that the circulation is far more complicated than that of the simple model, but nonetheless the potential vorticity distribution is dominated by f. Complications in the circulation theory may arise because the circulation at depths shallower than 2500 meters in β-dominated regions coexists with the wind-driven circulation which severely distorts the potential vorticity field; at depths greater than 2500 meters, topography is important since stratification is low (Warren and Owens, 1985). Abyssal heating should also influence this layer: zonal averages of potential vorticity on isopycnals below 3500 meters indicate that the meridional gradient in potential vorticity is less than β, suggesting that some type of bottom influence is active.

In summary, the potential vorticity distribution in the North Pacific has been found to be roughly consistent with recent theoretical ideas about the general circulation although there are a number of theoretical problems which have not yet been addressed. The distribution is also consistent with previous analyses of the North Pacific circulation, but has revealed some hitherto unrecognized features. The most definitive are the existence of subpolar mode waters of the sort previously reported in the North Atlantic (McCartney and Talley, 1982; McCartney, 1982) and the existence of

low potential vorticity at the top of the water column in the eastern Pacific. The correspondence of extrema of Ekman pumping and heat flux with potential vorticity extrema at shallow depths was also noted. Finally, the maps, sections, zonal averages, and schematic of the vertical–meridional structure of the potential vorticity field show distinct regions which can be identified with the predictions of various theories of wind-driven circulation and with thermohaline mechanisms.

Acknowledgments. This work was supported by the Office of Naval Research, Contract N00014-84-C-0218 to Oregon State University and by the Ocean Sciences Division of the National Science Foundation under Grants OCE831-6930 to Oregon State University and OCE84-16211 to Scripps Institution of Oceanography. Assistance from S. Gard (OSU) and M. Martin (SIO) in computing and preparation of materials and from S. Austensen and E. Spencer (SIO) in preparation of the manuscript was greatly appreciated. Comments from the anonymous reviewers were very helpful.

REFERENCES

Barkley, R. A., 1968: *Oceanographic Atlas of the Pacific Ocean,* University of Hawaii Press, (185 figures).

Coats, D. A., 1981: An estimate of absolute geostrophic velocity from the density field in the northeastern Pacific Ocean. *J. Geophys. Res.,* **86,** 8031–8036.

Cox, M. D., 1985: An eddy resolving numerical model of the ventilated thermocline. *J. Phys. Oceanogr.,* **15,** 1312–1324.

——, and K. Bryan, 1984: A numerical model of the ventilated thermocline. *J. Phys. Oceanogr.,* **14,** 674–687.

deSzoeke, R. A., 1987: On the wind-driven circulation of the South Pacific Ocean. *J. Phys. Oceanogr.,* **17,** 613–630.

Dewar, W. K., 1986: On the potential vorticity structure of weakly ventilated isopycnals: a theory of subtropical mode water maintenance. *J. Phys. Oceanogr.,* **16,** 1204–1216.

Dodimead, A. J., F. Favorite and T. Hirano, 1963: Salmon of the North Pacific Ocean. Part II. Review of oceanography of the subarctic Pacific region. *Int. North Pacific Fisheries Comm. Bull.,* **13,** 195 pp.

Fine, R. A., J. L. Reid and H. G. Ostlund, 1981: Circulation of tritium in the Pacific Ocean. *J. Phys. Oceanogr.,* **11,** 3–14.

Gill, A. E., 1982: *Atmosphere-Ocean Dynamics,* Academic Press, 662 pp.

Han, Y.-J., and S.-W. Lee, 1981: A new analysis of monthly mean wind stress over the global ocean, *Climatic Research Institute,* Rep. No. 26, Oregon State University, 148 pp.

Holland, W. R., T. Keffer and P. B. Rhines, 1984: Dynamics of the oceanic general circulation: the potential vorticity field. *Nature,* **308,** 698–705.

Huang, R. X., 1987: A three-layer model for wind-driven circulation in a subtropical/subpolar basin. Part II: The supercritical and hypercritical states. *J. Phys. Oceanogr.,* **17,** 679–692.

Jenkins, W. J., 1987: ^{3}H and ^{3}He in the Beta Triangle: observations of gyre ventilation and oxygen utilization rates. *J. Phys. Oceanogr.,* **17,** 763–783.

Joyce, T. M., B. A. Warren and L. D. Talley, 1986: The geothermal heating of the abyssal subarctic Pacific Ocean. *Deep-Sea Res.,* **33,** 1003–1015.

Keffer, T., 1985: The ventilation of the world's oceans: maps of the potential vorticity field. *J. Phys. Oceanogr.,* **15,** 509–523.

Levitus, S., 1982: Climatological atlas of the world ocean. NOAA Prof. Paper 13, 173 pp.

Luyten, J. R., J. Pedlosky and H. Stommel, 1983: The ventilated thermocline. *J. Phys. Oceanogr.,* **13,** 292–309.

Masuzawa, J., 1969: Subtropical mode water. *Deep-Sea Res.,* **16,** 463–472.

McCartney, M. S., 1977: Subantarctic mode water. *A Voyage of Discovery,* M. Angel, Ed., Pergamon Press, 103–119.

——, 1982: The subtropical recirculation of Mode Waters. *J. Mar. Res.,* **40**(Suppl.), 427–464.

——, and L. D. Talley, 1982: The subpolar mode water of the North Atlantic Ocean. *J. Phys. Oceanogr.,* **12,** 1169–1188.

McDowell, S., P. Rhines and T. Keffer, 1982: North Atlantic potential vorticity and its relation to the general circulation. *J. Phys. Oceanogr.,* **12,** 1417–1436.

Parsons, A. T., 1969: A two-layer model of Gulf Stream separation. *J. Fluid Mech.,* **39,** 511–528.

Pedlosky, J., and W. R. Young, 1983: Ventilation, potential-vorticity homogenization and the structure of the ocean circulation. *J. Phys. Oceanogr.,* **13,** 2020–2037.

——, W. Smith and J. R. Luyten, 1984: On the dynamics of the coupled mixed layer–thermocline system and the determination of the oceanic surface density. *J. Phys. Oceanogr.,* **14,** 1159–1171.

Reid, J. L., 1965: *Intermediate waters of the Pacific Ocean,* Johns Hopkins Press, 85 pp.

——, 1969: Sea-surface temperature, salinity, and density of the Pacific Ocean in summer and in winter. *Deep-Sea Res.,* **16**(Suppl.), 215–224.

——, 1982: On the use of dissolved oxygen concentration as an indicator of winter convection. *Naval Res. Rev.,* **34,** 28–39.

——, and R. S. Arthur, 1975: Interpretation of maps of geopotential anomaly for the deep Pacific Ocean. *J. Mar. Res.,* **33**(Suppl.), 37–52.

——, and A. W. Mantyla, 1978: On the mid-depth circulation of the North Pacific Ocean. *J. Phys. Oceanogr.,* **8,** 946–951.

Rhines, P. B., 1986: Vorticity dynamics of the oceanic general circulation. *Ann. Rev. Fluid Mech.,* **18,** 433–497.

——, and W. R. Young, 1982: A theory of wind-driven circulation 1. Mid-ocean gyres. *J. Mar. Res.,* **40**(Suppl.), 559–596.

Stommel, H., and A. B. Arons, 1960: On the abyssal circulation of the world ocean. I. Stationary planetary flow patterns on a sphere. *Deep-Sea Res.,* **6,** 140–154.

Talley, L. D., 1984: Meridional heat transport in the Pacific Ocean. *J. Phys. Oceanogr.,* **14,** 231–241.

——, 1985: Ventilation of the subtropical North Pacific: the shallow salinity minimum. *J. Phys. Oceanogr.,* **15,** 633–649.

——, and M. S. McCartney, 1982: Distribution and circulation of Labrador Sea Water. *J. Phys. Oceanogr.,* **12,** 1189–1205.

——, and M. E. Raymer, 1982: Eighteen Degree Water variability. *J. Mar. Res.,* **40**(Suppl.), 757–775.

——, and R. A. deSzoeke, 1986: Spatial fluctuations north of the Hawaiian Ridge. *J. Phys. Oceanogr.,* **16,** 981–984.

Tsuchiya, M., 1968: *Upper waters of the intertropical Pacific Ocean.* Johns Hopkins Press, 55 pp.

Young, W. R., and P. B. Rhines, 1982: A theory of wind-driven circulation II. Gyres with western boundary layers. *J. Mar. Res.,* **40,** 849–872.

Warren, B. A., and W. B. Owens, 1985: Some preliminary results concerning deep northern-boundary currents in the North Pacific. *Prog. Oceanogr.,* **14,** 537–551.

Wyrtki, K., and G. Meyers, 1976: The trade wind field over the Pacific Ocean. *J. Appl. Meteor.,* **15,** 698–704.